



## Geochemistry

## An experimental study of lake water-sediment interaction rates

*Une étude expérimentale de taux d'interaction d'eau-sédiment de lac*Cherif Gherbi<sup>a</sup>, Lakhdar Bouabssa<sup>b</sup>, Eric H. Oelkers<sup>c,\*</sup><sup>a</sup>Département des sciences naturelles, École normale supérieure, BP 92 Kouba, 16050 Alger, Algeria<sup>b</sup>Département de géologie, faculté des sciences de la terre, université Badji-Mokhtar, BP 12, 23000 Annaba, Algeria<sup>c</sup>UMR 5563, géochimie biogéochimie expérimentale, université Paul-Sabatier/LMTG CNRS, 14, avenue Édouard-Belin, 31400 Toulouse, France

## ARTICLE INFO

## Article history:

Received 4 August 2009

Accepted after revision 1 December 2009

Available online 5 March 2010

Presented by Georges Pédro

## Keywords:

Oued Cherf

Dissolution

Algeria

## Mots-clés :

Oued Cherf

Dissolution

Algérie

## ABSTRACT

Dissolution rates of sediments obtained from the Oued Cherf reservoir were measured in closed-system batch reactors at 25 °C in fluids sampled concurrently from the same locations as the sediments. The BET surface areas of the sediments ranged from 16 to 45 m<sup>2</sup>/g and consisted primarily of quartz, calcite, and clay minerals. After a brief initial period, release rates of Si, Mg, Ca, Cl, SO<sub>4</sub>, and NO<sub>3</sub> from these sediments are approximately linear with time over the course of the experiments, which lasted from 3 to 5 months. BET surface area normalized Si release rates ranged from 10<sup>-17.4</sup> to 10<sup>-18.4</sup> mol/cm<sup>2</sup>/s. These release rates match closely Si release rates from quartz and clay minerals determined from laboratory dissolution rates reported in the literature. This coherence suggests that laboratory measured silicate dissolution rates can be used with confidence to predict the dissolution behavior of sediments in natural surface waters.

© 2010 Académie des sciences. Published by Elsevier Masson SAS. All rights reserved.

## R É S U M É

Les vitesses de dissolution de sédiments échantillonnés dans la retenue du barrage de l'Oued Cherf ont été mesurées à l'aide de réacteurs fermés à 25 °C. Les sédiments, qui présentent des surfaces spécifiques BET comprises entre 16 et 45 m<sup>2</sup>/g sont essentiellement constitués de quartz, calcite et de minéraux argileux. Les taux de départ de Si, Mg, Ca, SO<sub>4</sub> et NO<sub>3</sub> en solution sont approximativement constants lors de ces expériences qui ont duré de trois à cinq mois. Les vitesses de départ de Si en solution, normalisées à la surface BET des sédiments, sont comprises entre 10<sup>-17,4</sup> à 10<sup>-18,4</sup> mol/cm<sup>2</sup>/s. Ces vitesses sont en bon accord avec les vitesses expérimentales de libération de la silice à partir de quartz et d'argiles reportées dans la littérature. Ces résultats indiquent que les vitesses de dissolution mesurées en laboratoire peuvent être utilisées avec confiance pour prévoir la vitesse de dissolution des sédiments dans les eaux naturelles superficielles.

© 2010 Académie des sciences. Publié par Elsevier Masson SAS. Tous droits réservés.

## 1. Introduction

Despite the fact that they are commonly used for drinking water, recreation, irrigation, and fishing, there

have been surprisingly few studies looking at the effect of the sediment-water interaction on the chemistry of lakes and reservoirs. Several studies have focused on how sediment-lake water interaction could affect the availability of essential nutrients such as phosphorous (e.g. House, 2003; Lijklema, 1993; Smits and Vandermolen, 1993). Other studies have investigated how lake sediments can influence the aqueous concentration of toxic or trace

\* Corresponding author.

E-mail address: oelkers@lmtg.obs-mip.fr (E.H. Oelkers).

metals, such as mercury (Vandal et al., 1995; Wolfenden et al., 2005) and other heavy metals (Gonzalez et al., 2000; Owens et al., 2005). To date, little is available on the rates of dissolution of major elements into lakes. This study attempts to fill, in part, this knowledge gap through a series of controlled laboratory experiments investigating the dissolution rates of Oued Cherf lake sediments in its waters.

The geology near the Oued Cherf lake has been described in detail by Vila (1980). The region is composed of sedimentary rocks from Trias to Quaternary in age; these rocks are dominated by limestones, sandstones, evaporates, and marls. The Oued Cherf lake (Fig. 1), began to fill following completion of its dam in 1994. This lake has a total capacity of 160 million m<sup>3</sup> of water, which is intended primarily for the irrigation of 1700 hectares of farmland. The hydrology of the watershed is dominated by the Oued Cherf, Oued Settara, Oued Mellah Kebira and Oued Melleh Seghira rivers. The Oued Cherf river, which enters the lake from the southeast, is the most important. It has an average flow of 5 m<sup>3</sup>/s in winter and 0.02 m<sup>3</sup>/s in summer. The climate is semi-arid with an average annual rainfall of 300 mm. Temperatures average 27 °C in the summer and 5 °C in the winter. Annual evapotranspiration is estimated to be approximately 270 mm representing 90% of the total rainfall.

A large number of studies have been performed to quantify the dissolution rates of the major rock forming minerals from laboratory experiments (e.g. Brantley, 2008; Oelkers, 2001; Schott et al., 2009; Sverdrup, 1990; White and Brantley, 1995). The applicability of such studies to natural systems has been questioned, as 'field' based rates at times appear to be significantly lower than their laboratory based counterparts (e.g. Ganor et al., 2007;

White and Brantley, 2003). These differences may stem from a number of sources including the effects of reaction affinity and secondary minerals (e.g. Maher et al., 2009; Zhu, 2005; Zhu and Lu, 2009), mineral age (e.g. Hodson and Langan, 1999; White, 1995), and difficulties in quantifying mineral dissolution/precipitation rates in the field (e.g. Hacini et al., 2008). This study is motivated in part to aid in the further understanding of such differences by studying the dissolution rates of lake sediments in their coexisting fluids in the laboratory. Natural sediments are in many ways similar to the material used in laboratory dissolution experiments. Whereas laboratory dissolution rates are commonly performed on minerals that have been ground and cleaned, natural sediments are ground during their transport and regularly cleaned by their interaction with flowing fluids. By dissolving sediments in the fluids that coexisted with them in nature we can mimic as close as possible the dissolution rates of these sediments in the natural environment.

## 2. Methods

Experiments were performed in 120 ml closed-system batch reactors similar to those described by Harouiya et al. (2007). Approximately 0.5 g of sediment was placed into each reactor, together with ~80 ml of the corresponding lake water sample. These reactors were sealed and placed a 25 °C temperature controlled oven. Each reactor was shaken by hand every 48 hours. Fluid samples were regularly taken from these reactors through 0.45 µm Millipore Nitrocellulose filters and stored till analysis.

The sediments used in these experiments were obtained by direct sampling from the bottom of the Oued Cherf near the lake edge; sample locations are shown in

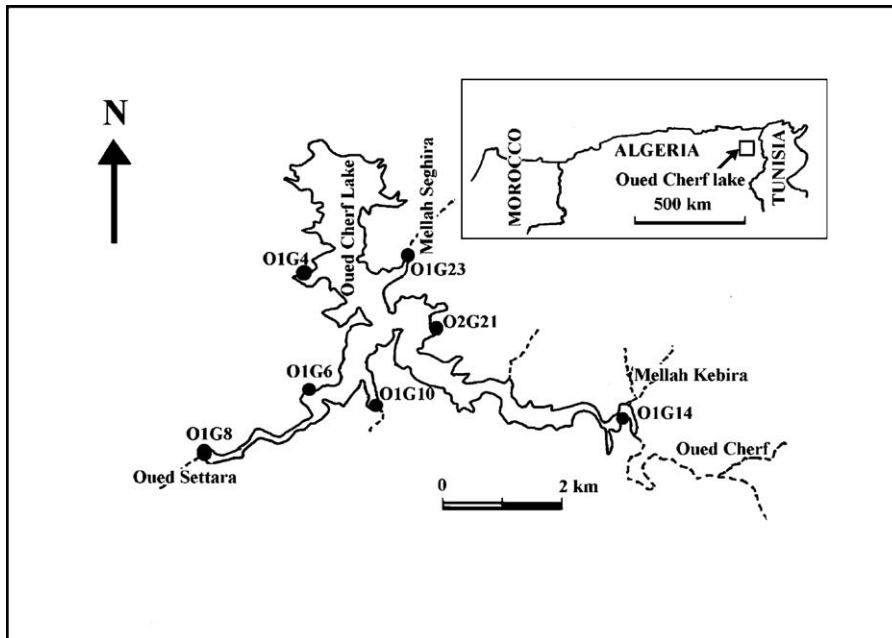
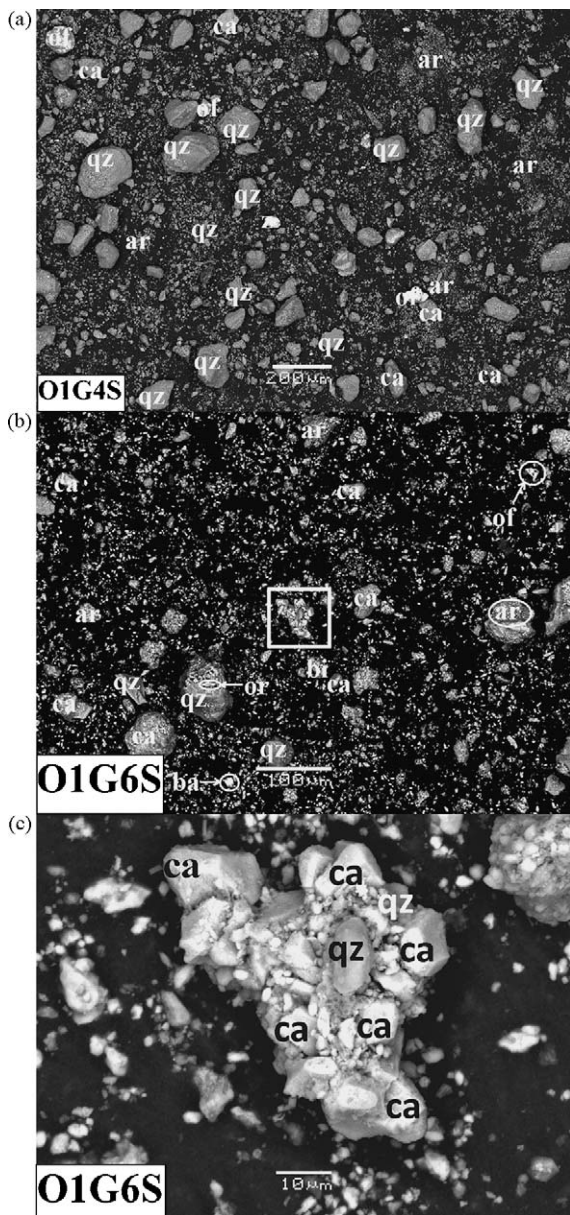


Fig. 1. Location of the samples collected within the Oued Cherf Lake in the present study.

Fig. 1. Localisation des échantillons prélevés dans le barrage d'Oued Cherf lors de la présente étude.



**Fig. 2.** SEM photomicrographs of two of the sediment samples dissolved in the present study: a) Sample O1G4S, b) Sample O1G6S, c) an enlargement of the boxed section of b. The abbreviations on the figure correspond to the identity of the mineral grains: qz = quartz, ca = calcite, of = iron oxide, ar = clays, ba = barite, bi = biotite.

**Fig. 2.** Images MEB de deux des échantillons de sédiments mis en solution au cours de cette étude : a) Echantillon O1G4S, b) Echantillon O1G6S, c) Détail de la zone encadrée b. Les abréviations sur la figure correspondent aux noms des minéraux : qz = quartz, ca = calcite, of = oxydes de fer, ar = argiles, ba = barite, bi = biotite.

**Fig. 1.** These sediments were air dried and used in these experiments without further preparation. The dried sediments were characterized by X-ray diffraction, scanning electron microscopy (SEM), and X-ray fluorescence. X-ray diffraction measurements, performed using an INCEL CPS 120 diffractometer with Coradiation ( $\lambda = 1.78 \text{ \AA}$ ), indicates that these sediments are comprised

of quartz, calcite, clay minerals, and minor iron oxides and sulfate minerals. SEM images of some of the sediments, obtained using a JEOL JSM-6360LV Scanning Electron Microscope, are shown in Fig. 2. The sediments consist of grains that are less than  $100 \mu\text{m}$  in size, the bulk of the grains are considerably smaller. Some of the larger grains are agglomerates containing particles of various minerals. The chemical compositions of these solids as determined by X-ray fluorescence using a Panalytical PW2400 are shown in Table 1. The compositions vary considerably sample to sample; the  $\text{SiO}_2$  content of these samples range from 18 to 78%. The surface area of these sediments was determined by the three-point BET method (Brunauer et al., 1938) using  $\text{N}_2$  gas. The results of these analyses are summarized in Table 1; surface areas range from 16 to  $45 \text{ cm}^2/\text{g}$ .

The aqueous solutions used for the experiments were obtained from the same locations as the sediment samples as noted by the locations shown in Fig. 1. These aqueous solutions were collected in acid washed bottles and filtered through  $0.45 \mu\text{m}$  Millipore Nitrocellulose filters prior to their use in the experiments. The composition of these solutions, as well as those collected during the experiments were determined by atomic absorption spectroscopy (AAS) with an uncertainty of  $\pm 1\%$  and a detection limit of  $6 \times 10^{-7} \text{ M}$ , and ion chromatography using Dionex High Pressure Liquid Chromatograph (HPLC) with a precision of better than 8%. Alkalinity was determined by standard HCl titration with an uncertainty of  $\pm 1\%$  and a detection limit of  $5 \times 10^{-5} \text{ M}$ . pH of all aqueous solutions was measured at  $25^\circ\text{C}$  using a standard glass electrode. These measurements have a  $\pm 0.02$  uncertainty in pH. The pH measured in the laboratory is within 0.03 pH units of those measured originally in the field. The composition of the initial aqueous solutions is listed in Table 2.

The saturation state of various mineral phases in these aqueous solutions was investigated via the PHREEQC (Parkhurst and Appelo, 1999) together with its LLNL database<sup>1</sup>. The results of these calculations are shown in Table 3. These solutions are close to equilibrium with respect to quartz and calcite, the minerals that dominate the sediments. These natural solutions are also undersaturated with respect to the sulfates gypsum and anhydrite, and various evaporate minerals (e.g. epsomite, hexahydrate). Interestingly calculations suggest these lake fluids are supersaturated with respect to the Al-oxihydroxide diaspore and the primary Al-silicate phases K-feldspar, kaolinite, and muscovite. This later results could stem from an overestimate in the activity of aqueous Al due to lack of characterization of potential Al-ligand complexes in solution.

### 3. Results

The temporal evolution of the aqueous phase composition during all closed-system experiments are listed in

<sup>1</sup> The database used in the present study has the id: llnl.dat 85 2005-02-02. The data for this database were taken from 'thermo-com.V8.R6.230' prepared by Jim Johnson at Lawrence Livermore National Laboratory.

**Table 1**  
Composition of solids used in the present study determined by X-ray fluorescence.

**Tableau 1**  
Composition des solides utilisés dans la présente étude, déterminée par fluorescence X.

% Oxides	O1G04S	O1G06S	O1G08S	O1G10S	O1G14S	O1G23S	O2G21S
SiO <sub>2</sub>	77.89	31.77	35.74	18.17	44.85	57.89	48.1
Al <sub>2</sub> O <sub>3</sub>	3.44	3.38	11.79	4.57	15.00	9.35	5.41
Fe <sub>2</sub> O <sub>3</sub>	3.21	4.35	5.71	2.62	7.34	7.08	4.74
MnO	0.03	0.08	0.06	0.03	0.08	0.18	0.09
MgO	–	0.59	1.47	0.87	1.86	1.65	1.08
CaO	7.73	32.11	19.59	50.56	23.3	7.13	22.21
Na <sub>2</sub> O	–	–	–	–	2.1	1.51	–
K <sub>2</sub> O	0.4	0.5	0.81	0.67	1.7	1.29	0.82
P <sub>2</sub> O <sub>5</sub>	0.06	0.08	0.14	0.04	0.18	0.15	0.09
TiO <sub>2</sub>	0.3	0.27	0.58	0.35	–	0.66	0.45
PP <sup>a</sup>	6.2	26.23	23.4	21.7	2.2	10.5	16.3
Cl	–	0.02	0.08	–	1.05	0.96	0.09
Total	99.26	99.36	99.29	99.58	98.61	97.39	99.29
S.A <sup>b</sup>	15.69	16.46	44.97	30.07	47.21	15.79	38.9

<sup>a</sup> Loss on ignition.

<sup>b</sup> Surface area (m<sup>2</sup>/g).

**Table 2**  
Composition of initial aqueous solutions used in the present study.

**Tableau 2**  
Composition des solutions initiales utilisées dans la présente étude.

Anions/cations	O1G04E	O1G06E	O1G08E	O1G10E	O1G14'E	O1G23E	O2G21E
Na (ppm)	313.31	344.99	317.83	321.06	327.32	348.66	368.07
Mg (ppm)	57.42	58.32	60.54	56.92	57.24	58.21	61.83
Cl (ppm)	490.21	506.64	481.07	470.30	490.82	504.46	517.38
K (ppm)	20.92	24.56	18.98	19.87	19.78	20.35	19.90
Ca (ppm)	129.96	125.59	141.36	133.88	155.49	147.33	149.02
SO <sub>4</sub> (ppm)	296.73	309.50	304.70	285.86	292.17	338.18	334.49
HCO <sub>3</sub> (mmol/l)	1.80	1.56	2.93	2.12	3.15	2.56	2.50
NO <sub>3</sub> (ppm)	32.81	33.45	38.71	33.63	32.09	34.69	24.38
Si (ppm)	1.63	1.67	2.22	1.64	1.64	1.77	1.35
Al (ppb)	0.78	1.72	4.03	0.33	2.00	15.53	1.16
pH	7.75	8.10	8.05	8.05	7.95	7.90	7.70

**Table 4.** The solutions sampled during each experiment are denoted sequentially by the number in parentheses in this table. The concentrations of a number of elements changed substantially at the onset of the experiments. The aqueous concentrations of Na, K, Al, Si, Cl, and SO<sub>4</sub> tend to increase notably once the sediments are introduced into the lake water. In contrast, the aqueous concentration of calcium dropped appreciably during the first few minutes of each experiment. The initial release of NO<sub>3</sub> and alkalinity to aqueous solution shows no clear trend.

Following this initial period the aqueous concentrations of Si, Ca, Na, Mg, Cl, SO<sub>4</sub>, and NO<sub>3</sub> increase systematically with time, which is consistent with mineral dissolution. To quantify the release rates of these elements, the mass of each element in the total fluid phase of each experiment (equal to the element present in the fluid in the reactor and that in the fluids sampled previously from the reactor) was determined from

$$M_i = c_{i,r} V_r + \sum_n c_{i,n} V_n \quad (1)$$

where  $M_i$  stands for the mass of the  $i$ th element in the fluid phase,  $c_{i,r}$  corresponds to the concentration of this element in the fluid phase present in the reactor,  $c_{i,n}$

represents this concentration in the  $n$ th fluid sample, and  $V_r$  and  $V_n$  denote the mass of fluid present in the reactor and taken during the  $n$ th sample, respectively. Masses of elements present in the aqueous phase from the latter part of three representative experiments are presented in Fig. 3. Element release rates ( $r_i$ ) were obtained from these masses using

$$r_i = \frac{1}{S_{BET}} \frac{\partial M_i}{\partial t} \quad (2)$$

where  $t$  denotes time, and  $S_{BET}$  corresponds to the BET surface area of the sediments present in the reactor. Linear regressions of  $M_i$  versus time were performed on all experiments performed in this study. Examples of these regressions are shown in Fig. 3. These regressions were made on the final 5–7 fluid samples from each experiment to avoid the initial effects described above. For the most part these linear regressions provide an excellent description of the temporal evolution of  $M_i$ . In some cases, however, the distributions of aqueous concentrations exhibit a decrease in slope with time during the experiments, consistent with slowing dissolution rates. The slowing of dissolution rates could stem from an approach

**Table 3**

Saturation state of initial and final fluids of all experiments with respect to selected phases calculated using PHREEQC (Parkhurst and Appelo, 1999) together with its LLNL database. .

**Tableau 3**

Etat de saturation des solutions initiales et finales des expériences en tenant compte des phases calculées à l'aide de PHREEQC (Parkhurst et Appelo, 1999) avec sa base des données LLNL.

Phases	O1G4E(0)	O1G4E(6)	O1G6E(0)	O1G6E(7)	O1G8E(0)	O1G8E(7)	O1G10E(0)	O1G10E(7)	O1G14'E(0)	O1G14'E(7)	O1G23E(0)	O1G23E(7)	O2G21E(0)	O2G21E(7)
Albite	-1.43	0.03	-1.07	-0.02	-0.67	0.55	-1.77	1.07	-1.38	0.46	-0.43	-0.31	-1.68	-0.02
Amesite-14A	-3.88	5.20	-1.02	4.62	0.71	6.00	-4.16	6.12	-1.27	5.88	2.18	2.85	-3.41	5.48
Analcime	-1.45	0.02	-1.13	-0.04	-0.78	0.37	-1.81	0.80	-1.35	0.32	-0.45	-0.39	-1.61	0.02
Anhydrite	-1.45	-1.19	-1.44	-1.25	-1.37	-1.20	-1.44	-1.21	-1.35	-1.17	-1.30	-1.22	-1.33	-1.20
Anorthite	-6.96	-3.53	-6.20	-3.63	-5.32	-3.10	-7.57	-2.46	-6.15	-3.25	-4.37	-4.70	-6.77	-3.43
Aragonite	-0.00	0.49	0.27	0.30	0.60	0.61	0.37	0.15	0.57	0.75	0.42	0.46	0.16	0.52
Boehmite	0.27	1.39	0.33	1.43	0.58	1.36	-0.30	1.85	0.37	1.26	1.27	0.68	0.45	1.49
Calcite	0.15	0.63	0.42	0.45	0.75	0.75	0.52	0.30	0.72	0.89	0.56	0.60	0.31	0.67
Chrysotile	-2.88	0.42	-0.86	-0.14	-0.36	1.19	-1.32	-0.15	-1.29	1.40	-1.40	0.83	-3.13	0.31
Clinochlore-14A	-3.18	4.64	0.27	3.79	1.62	5.81	-1.76	4.53	-0.30	5.96	1.31	3.87	-3.20	4.66
Clinochlore-7A	-6.62	1.26	-3.18	0.41	-1.79	2.43	-5.22	1.15	-3.71	2.58	-2.09	0.50	-6.64	1.29
Dawsonite	-1.14	-0.09	-1.22	-0.17	-0.80	-0.12	-1.73	0.20	-0.99	-0.08	-0.16	-0.81	-0.93	0.04
Diaspore	0.69	1.80	0.74	1.84	0.99	1.77	0.12	2.26	0.78	1.66	1.68	1.08	0.87	1.89
Diopside	-4.74	-2.56	-3.40	-2.94	-2.98	-1.93	-3.67	-2.77	-3.62	-1.78	-3.71	-2.23	-4.94	-2.67
Dolomite	1.28	2.30	1.84	1.95	2.48	2.55	2.00	1.64	2.36	2.78	2.08	2.26	1.58	2.37
Epsomite	-3.89	-3.72	-3.84	-3.75	-3.86	-3.72	-3.88	-3.73	-3.90	-3.75	-3.84	-3.73	-3.82	-3.73
Gibbsite	0.14	1.20	0.19	1.24	0.42	1.17	-0.42	1.66	0.21	1.07	1.10	0.49	0.31	1.30
Gypsum	-1.19	-1.0	-1.16	-1.06	-1.14	-1.02	-1.16	-1.03	-1.12	-0.99	-1.08	-1.04	-1.08	-1.02
Hexahydrite	-4.12	-3.95	-4.08	-3.99	-4.09	-3.96	-4.11	-3.97	-4.14	-3.98	-4.08	-3.97	-4.05	-3.96
Illite	0.51	3.15	1.14	3.02	1.81	3.70	-0.36	4.96	0.77	3.38	2.84	1.80	0.52	3.03
K-Feldspar	0.34	1.37	0.89	1.07	1.12	1.83	0.17	2.51	0.44	1.68	1.34	0.83	0.14	1.04
Kaolinite	0.83	2.83	0.99	2.95	1.55	3.12	-0.22	4.27	0.88	2.82	2.69	1.60	0.97	2.93
Magnesite	-0.54	0.05	-0.26	-0.12	0.08	0.17	-0.20	0.29	-0.01	0.26	-0.13	0.03	-0.39	0.08
Montmor-Ca	0.46	2.51	0.98	2.55	1.62	3.22	-0.07	4.13	0.66	2.92	2.18	1.74	0.34	2.47
Montmor-K	0.23	2.16	0.78	2.10	1.35	2.83	-0.29	3.80	0.39	2.54	1.91	1.33	0.09	2.02
Montmor-Mg	0.54	2.60	1.06	2.64	1.70	3.31	0.00	4.22	0.73	3.00	2.25	1.83	0.41	2.56
Montmor-Na	0.33	2.38	0.82	2.40	1.44	3.07	-0.25	3.99	0.46	2.80	1.99	1.62	0.17	2.34
Muscovite	2.20	5.43	2.85	5.21	3.58	5.83	0.89	7.49	2.48	5.46	5.17	3.46	2.35	5.30
Nesquehonite	-3.58	-2.97	-3.31	-3.14	-2.95	-2.85	-3.26	-3.30	-3.04	-2.76	-3.15	-2.98	-3.43	-2.94
Paragonite	-0.49	3.19	-0.03	3.22	0.87	3.65	-1.96	5.15	-0.25	3.35	2.49	1.42	-0.38	3.34
Pentahydrite	-4.46	-4.29	-4.42	-4.33	-4.43	-4.30	-4.45	-4.30	-4.48	-4.32	-4.42	-4.31	-4.39	-4.30
Phlogopite	-1.05	3.48	1.46	2.58	2.12	4.36	0.25	3.53	0.77	4.50	1.53	3.16	-1.29	3.14
Pyrophyllite	-0.97	0.93	-0.76	1.08	-0.08	1.56	-1.95	2.88	-1.02	1.17	0.83	-0.11	-1.02	0.92
Quartz	-0.05	-0.14	-0.02	-0.12	0.02	0.03	-0.00	0.12	-0.11	-0.01	-0.10	-0.04	-0.15	-0.19
Sepiolite	-6.15	-2.17	-3.36	-2.86	-2.62	-0.57	-3.90	-2.09	-4.29	-0.45	-4.41	-1.31	-6.85	-2.50



**Table 4**

Evolution of the aqueous solution compositions during the experiments performed in the present study.

**Tableau 4**

Évolution de la composition des solutions lors des expériences menées dans cette étude.

O1G4S+O1G4E	O1G4E(0)	O1G4E(1)	O1G4E(2)	O1G4E(3)	O1G4E(4)	O1G4E(5)	O1G4E(6)	O1G4E(6)
Time (s)	0.00E+00	3.07E+05	5.70E+05	1.29E+06	2.59E+06	5.26E+06	7.83E+06	7.83E+06
pH	8.05	7.97	7.95	7.96	8.03	8.14	8.09	8.09
Si (ppm)	1.63	1.73	1.74	1.77	1.76	1.79	1.96	1.96
Ca (ppm)	129.96	121.13	121.46	122.65	118.14	135.45	145.54	145.54
Na (ppm)	313.31	334.99	322.71	323.75	359.44	369.22	399.83	399.83
K (ppm)	20.92	46.44	21.78	19.13	16.68	17.24	13.66	13.66
Mg (ppm)	57.42	58.08	54.41	55.58	57.00	61.14	68.18	68.18
Cl (ppm)	490.21	595.35	581.03	580.63	599.70	623.11	700.21	700.21
SO <sub>4</sub> (ppm)	296.73	388.26	386.85	388.38	402.85	418.14	457.53	457.53
NO <sub>3</sub> (ppm)	32.81	32.45	32.44	33.84	35.03	37.11	45.14	45.14
Alc, (mol/l)	1.80E-03	2.00E-03	1.93E-03	1.94E-03	1.92E-03	1.92E-03	1.86E-03	1.86E-03
Al (ppb)	0.78	45.22	50.22	51.73	44.73	48.98	45.95	45.95
O1G6E+O1G6S	O1G6E(0)	O1G6E(1)	O1G6E(2)	O1G6E(3)	O1G6E(4)	O1G6E(5)	O1G6E(6)	O1G6E(7)
Time (s)	0.00E+00	8.88E+04	1.74E+05	1.04E+06	2.34E+06	4.93E+06	7.61E+06	1.02E+07
pH	8.08	7.99	8.00	7.94	7.94	7.81	7.98	8.00
Si (ppm)	1.67	1.70	1.71	1.73	1.78	1.78	1.86	2.03
Ca (ppm)	127.04	116.41	117.20	115.92	116.66	122.80	123.01	130.62
Na (ppm)	334.82	337.61	330.02	329.99	334.58	342.90	351.54	346.71
K (ppm)	24.56	61.45	43.25	72.80	61.36	12.73	14.58	6.74
Mg (ppm)	58.32	59.52	56.62	56.16	57.92	57.66	60.21	63.75
Cl (ppm)	506.64	601.00	616.56	627.24	617.67	589.99	602.94	626.81
SO <sub>4</sub> (ppm)	309.50	387.64	396.49	398.37	390.61	397.74	405.93	421.68
NO <sub>3</sub> (ppm)	33.45	32.76	33.50	34.13	33.00	34.13	34.71	36.94
Alc, (mol/l)	1.56E-03	1.66E-03	1.65E-03	1.62E-03	1.62E-03	1.59E-03	1.64E-03	1.59E-03
Al (ppb)	1.72	31.99	31.99	34.28	35.39	35.73	36.30	41.05
O1G8S+O1G8E	O1G8E(0)	O1G8E(1)	O1G8E(2)	O1G8E(3)	O1G8E(4)	O1G8E(5)	O1G8E(6)	O1G8E(7)
Time (s)	0.00E+00	2.54E+05	5.16E+05	1.23E+06	2.53E+06	5.21E+06	7.77E+06	1.04E+07
pH	8.36	8.09	8.11	8.16	8.11	8.12	8.13	8.16
Si (ppm)	2.22	2.64	2.63	2.78	2.75	2.78	2.89	2.93
Ca (ppm)	141.36	139.96	131.36	138.00	142.14	140.41	140.62	145.33
Na (ppm)	317.83	323.84	324.80	331.44	336.76	341.01	350.97	359.04
K (ppm)	18.98	44.32	16.01	17.49	14.80	15.51	9.91	10.79
Mg (ppm)	60.54	61.79	58.65	58.56	58.95	61.18	65.78	67.77
Cl (ppm)	481.07	589.64	565.37	576.89	573.07	594.72	596.37	645.21
SO <sub>4</sub> (ppm)	304.70	393.85	391.18	399.85	399.68	415.22	415.89	442.29
NO <sub>3</sub> (ppm)	38.71	38.67	38.56	40.00	40.57	41.31	43.96	48.33
Alc, (mol/l)	2.93E-03	3.06E-03	3.05E-03	2.97E-03	2.83E-03	2.72E-03	2.43E-03	2.07E-03
Al (ppb)	4.03	45.13	48.88	43.81	50.11	46.41	43.41	50.12
O1G10S+O1G10E	O1G10E(0)	O1G10E(1)	O1G10E(2)	O1G10E(3)	O1G10E(4)	O1G10E(5)	O1G10E(6)	O1G10E(7)
Time (s)	0.00E+00	3.07E+05	5.68E+05	1.29E+06	2.58E+06	5.26E+06	7.83E+06	1.04E+07
pH	8.01	7.84	7.92	7.92	7.82	7.83	7.89	7.91
Si (ppm)	1.64	2.57	2.77	2.84	2.96	3.16	3.17	3.50
Ca (ppm)	133.88	120.67	118.72	115.95	122.57	125.79	135.97	143.50
Na (ppm)	321.06	328.49	329.51	324.55	333.86	356.90	348.43	387.71
K (ppm)	19.87	50.01	21.29	17.84	17.57	18.53	12.21	16.67
Mg (ppm)	56.92	58.31	54.63	55.17	55.73	51.02	60.69	67.26
Cl (ppm)	470.30	596.16	590.10	581.82	598.33	614.01	605.40	684.46
SO <sub>4</sub> (ppm)	285.86	389.31	392.25	390.33	401.50	412.03	404.21	442.82
NO <sub>3</sub> (ppm)	33.63	32.85	35.47	32.78	34.30	34.78	34.70	41.27
Alc, (mol/l)	2.12E-03	1.68E-03	1.64E-03	1.61E-03	1.56E-03	1.56E-03	1.45E-03	1.30E-03
Al (ppb)	0.33	90.98	84.43	87.14	86.28	84.58	82.88	88.75
O1G14S+O1G14'E	O1G14'E(0)	O1G14'E(1)	O1G14'E(2)	O1G14'E(3)	O1G14'E(4)	O1G14'E(5)	O1G14'E(6)	O1G14'E(7)
Time (s)	0.00E+00	2.53E+05	5.15E+05	1.24E+06	2.54E+06	5.21E+06	7.77E+06	1.04E+07
pH	8.41	8.18	8.18	8.19	8.12	8.15	8.19	8.22
Si (ppm)	1.64	2.04	2.06	2.27	2.37	2.50	2.61	2.66
Ca (ppm)	155.49	144.03	116.86	145.18	148.42	151.68	153.93	159.22
Na (ppm)	327.32	379.53	327.09	390.55	376.73	396.88	502.28	447.17
K (ppm)	19.78	32.11	12.73	20.89	16.26	16.10	10.27	11.62
Mg (ppm)	57.24	57.27	46.88	55.09	56.05	58.63	66.91	66.04
Cl (ppm)	490.82	645.83	542.49	631.53	657.86	660.80	677.12	748.44
SO <sub>4</sub> (ppm)	292.17	398.80	339.67	395.00	413.43	414.79	421.80	456.65
NO <sub>3</sub> (ppm)	32.09	37.36	32.13	37.54	40.32	41.21	43.38	49.88

**Table 4** (Continued)

O1G14S+O1G14E	O1G14E(0)	O1G14E(1)	O1G14E(2)	O1G14E(3)	O1G14E(4)	O1G14E(5)	O1G14E(6)	O1G14E(7)
Alc. (mol/l)	3.15E-03	3.33E-03	3.13E-03	3.08E-03	3.07E-03	3.05E-03	2.76E-03	2.38E-03
Al (ppb)	2.00	45.08	42.64	43.83	43.46	43.14	45.50	45.56
O1G23S+O1G23E	O1G23E(0)	O1G23E(1)	O1G23E(2)	O1G23E(3)	O1G23E(4)	O1G23E(5)	O1G23E(6)	O1G23E(7)
Time (s)	0.00E+00	2.39E+05	5.02E+05	1.22E+06	2.52E+06	5.19E+06	7.76E+06	1.03E+07
pH	8.16	8.10	8.11	8.13	8.07	8.11	8.10	8.13
Si (ppm)	1.77	1.93	1.99	2.09	2.11	2.25	2.44	2.45
Ca (ppm)	147.33	136.97	132.75	132.64	140.11	140.52	139.59	140.89
Na (ppm)	348.66	389.45	393.65	432.92	395.13	405.90	414.47	439.05
K (ppm)	20.35	27.41	24.26	11.69	15.01	13.51	7.44	9.55
Mg (ppm)	58.21	60.01	57.65	56.80	58.53	48.80	63.87	67.38
Cl (ppm)	504.46	684.78	677.54	673.43	690.69	693.80	708.99	779.42
SO <sub>4</sub> (ppm)	338.18	411.33	409.06	408.35	419.05	420.60	424.47	450.71
NO <sub>3</sub> (ppm)	34.69	34.14	33.82	33.90	35.52	35.80	36.80	41.19
Alc. (mol/l)	2.56E-03	2.15E-03	2.12E-03	2.09E-03	2.02E-03	1.96E-03	1.86E-03	1.66E-03
Al (ppb)	15.53	10.10	9.21	10.49	9.70	11.07	9.62	9.81
O2G21E+O2G21S	O2G21E(0)	O2G21E(1)	O2G21E(2)	O2G21E(3)	O2G21E(4)	O2G21E(5)	O2G21E(6)	O2G21E(7)
Time (s)	0.00E+00	8.97E+04	1.73E+05	1.03E+06	2.34E+06	4.93E+06	7.61E+06	1.02E+07
pH	8.21	8.18	8.21	8.16	8.14	8.05	8.08	8.09
Si (ppm)	1.35	1.40	1.40	1.46	1.50	1.54	1.59	1.74
Ca (ppm)	149.02	142.93	145.26	142.36	140.08	140.30	141.75	146.35
Na (ppm)	368.07	415.53	388.54	380.53	402.93	369.63	373.38	404.86
K (ppm)	19.90	34.94	25.30	40.22	39.57	12.26	11.97	7.29
Mg (ppm)	61.83	58.47	59.48	58.24	59.95	59.91	62.12	67.57
Cl (ppm)	517.38	646.03	654.45	693.86	650.51	629.24	659.87	696.62
SO <sub>4</sub> (ppm)	334.49	411.57	415.66	427.51	410.54	412.52	432.65	451.15
NO <sub>3</sub> (ppm)	24.38	23.32	23.66	24.46	23.52	24.68	27.66	29.50
Alc. (mol/l)	2.50E-03	2.72E-03	2.73E-03	2.62E-03	2.56E-03	2.33E-03	2.30E-03	2.00E-03
Al (ppb)	1.16	44.09	45.04	54.79	59.93	60.79	58.56	57.67

to equilibrium of the aqueous fluid with respect to one or more minerals in the sediments (c.f. Schott and Oelkers, 1995). In such instances rates computed from the first two and last two measured aqueous concentrations in Fig. 3 differ from that of the regression curve by no more than a factor of 2. The slope of the regression curves in Fig. 3 corresponds to  $\partial Mi/\partial t$ . These slopes were used to calculate element release rates using Eq. (2). The results of this calculation are summarized in Table 5. Note that the evolution of aqueous Al concentration tend to remain nearly constant, likely due to the combination of the dissolution of Al-bearing phases coupled to Al-hydroxide precipitation. In contrast to the other elements, the long-term aqueous K concentrations and alkalinity tend to decrease throughout the experiments.

Calculated element release rates of Si, Ca, Na, Mg, Cl, SO<sub>4</sub>, and NO<sub>3</sub> are remarkably consistent experiment to experiment and element to element. Logarithms of Si

release rates in units of mol/cm<sup>2</sup>/s, vary only from –18.4 to –17.4; those of Mg vary only from –16.4 to –16.9. The fastest measured released element is Na, the logarithm of its release rates are as high as –15.8, which is less than three orders of magnitude faster than that of the slowest measured element release rate in this study.

#### 4. Discussion

The results presented above illustrate distinct behaviors between the initial and long-term element release rates into solution. At the onset of the closed-system experiments, the concentration of elements in the aqueous solution changed rapidly compared with their longer-term evolution. As these experiments consist of reacting lake sediments in the aqueous solutions collected simultaneously from the same locations it seems likely that this distinct initial behavior stems from the handling of the

**Table 5**

Logarithm of the rates of elements released to aqueous solution during the experiments performed in the present study.

**Tableau 5**

Logarithmes des vitesses de départ des éléments en solution lors des expériences menées dans la présente étude.

Log r (mol/cm <sup>2</sup> /s)	O1G4	O1G6	O1G8	O1G10	O1G14	O1G23	O2G21
Log r (Si)	–18.42	–17.75	–18.06	–17.53	–17.78	–17.43	–18.16
Log r (Ca)	–16.6	–16.22	–16.66	–16.49	–16.2	–16.25	–17.16
Log r (Na)	–15.9	–15.75	–15.96	–15.79	–16.38	–15.36	–16.64
Log r (Mg)	–16.6	–16.38	–16.66	–16.71	–16.38	–16.51	–16.94
Log r (Cl)	–15.9	–15.92	–15.96	–15.88	–15.68	–15.51	–15.94
Log r (SO <sub>4</sub> )	–16.42	–16.23	–16.66	–16.49	–16.2	–16.3	–16.64
Log r (NO <sub>3</sub> )	–17.12	–16.92	–17.18	–17.19	–16.84	–16.91	–17.16

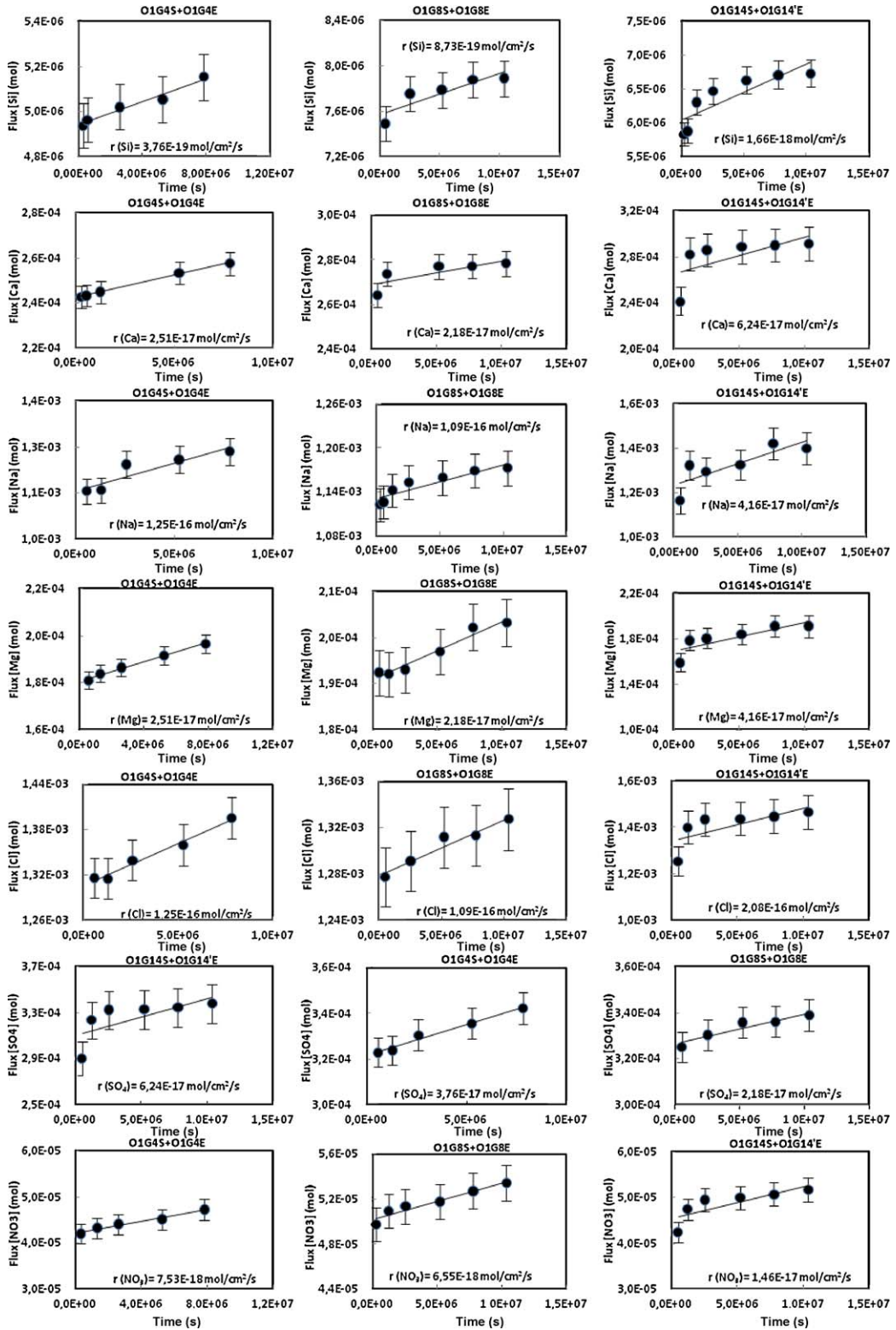


Fig. 3. Regression plots of the temporal evolution of major element fluxes into the reactive fluids during three representative experiments performed in the present study. The symbols correspond to measured fluxes, whereas the lines correspond to a linear least squares fit of these data. The element release rates consistent with these linear fits are provided on the plots.

Fig. 3. Variation en fonction du temps des flux des éléments vers les solutions réactives, lors de trois expériences représentatives. Les symboles correspondent aux flux mesurés et les courbes représentent les régressions linéaires des données. Les vitesses de départ des éléments déduits de ces courbes sont reportées dans la figure.



solutions and sediments between their collection and the beginning of the experiments. Three distinct processes that could contribute to the observed distinct initial behavior include:

- the partial or complete equilibration of the lake water samples with the atmosphere;
- the formation of soluble salts on the sediments during drying;
- the precipitation of insoluble phases in the aqueous solution.

It seems likely that each of these processes contributed to the initial behavior of the experiments described above. Ca drops notably during the initial part of each experiment consistent with calcite precipitation and the observation that calcite is supersaturated in the initial aqueous fluids. This supersaturation could have stemmed from interaction of the lake water with the atmosphere following its collection. The rapid initial release of Na, K, Si, Cl, and SO<sub>4</sub> suggests the rapid dissolution of soluble salts that could have formed during the drying of the sediments following their original sampling. The rapid rise in Al concentrations of the lake water could be due to Al hydroxide precipitation during the time between their sampling and their use in these experiments; note these lake samples are supersaturated with respect to diaspore. Once the experiments started, aqueous Al concentrations could increase due to the dissolution of Al-bearing phases (e.g. clay minerals).

The longer-term temporal variation of the aqueous phase composition stems from mineral reactions. The direct comparison of long-term element release rates determined above with dissolution and precipitation rates of individual minerals measured in the laboratory is challenging for a number of reasons. First, element release rates generated above are normalized to the surface area of the sediments whereas mineral dissolution/precipitation rates are normalized to the surface area of the individual minerals. It seems likely that the surface area of the sediments measured in the present study are dominated by those of clay minerals rather than that of other minerals present in the sediments (c.f. Sverdrup, 1990; Sverdrup and Warfvinge, 1993). Second, mineral dissolution rates depend strongly on saturation state and aqueous fluid composition (e.g. Oelkers, 2001; Schott et al., 2009). Accurate determination of the saturation state of many low-temperature minerals, such as clays, is challenging owing to current limitations in thermodynamic databases (Oelkers et al., 2009). Third, the mineral source of each element released into solution may be ambiguous as several minerals contain the same element.

Despite some of the challenges listed above, comparison between element release rates generated in this study with dissolution rates of individual minerals can provide insight into both lake water-sediment interaction and the degree to which one can use laboratory measured rates to model natural processes. One striking feature of the results of this study is that the long-term release rates of element measured in this study vary by only three orders of magnitude. This consistency contrasts with the large differences in the dissolution rates of the minerals

containing of Si, Ca, Na, Mg, Cl, SO<sub>4</sub>, and NO<sub>3</sub> present in the sediments as measured during laboratory experiments, which span by over 12 orders of magnitude. The near to neutral pH 'far-from-equilibrium' dissolution rates of halite are  $> 10^{-6}$  mol/(cm<sup>2</sup> s) (Alkattan et al., 1997), of barite are  $\sim 10^{-7.5}$  mol/(cm<sup>2</sup> s) (Dove and Czank, 1995), of calcite are  $\sim 10^{-9.8}$  mol/(cm<sup>2</sup> s) (e.g. Cubillas et al., 2005; Plummer et al., 1978), of quartz are  $\sim 10^{-17.7}$  mol/(cm<sup>2</sup> s) (Brady and Walther, 1990) and those of the clay minerals montmorillonite are  $\sim 10^{-18.2}$  mol/(cm<sup>2</sup> s) (Rozalen et al., 2008), kaolinite are  $\sim 10^{-18.2}$  mol/(cm<sup>2</sup> s) (Huertas et al., 1999) and illite are  $10^{-18.8}$  mol/(cm<sup>2</sup> s) (Köhler et al., 2003). Possible reasons why the element release rates measured in the sediments are similar to one another and similar to that of the slow dissolving minerals are that the rapidly dissolving minerals either:

- attain rapidly an equilibrium or close to equilibrium state, as appears to be the case for calcite;
- rapidly consume all accessible material, which is likely the case for halite.

Measured element release rates are, however, close to those of the slow dissolving minerals, quartz and clays, suggesting these minerals are controlling the chemical evolution of the aqueous phase during our experiments. Nevertheless, the aqueous phase is close to equilibrium with respect to quartz, and supersaturated with respect to a large number of clay phases. It is, therefore, difficult to determine which phase dominates the overall dissolution of the sediments. As many of the sediment grains are agglomerates of a number of minerals, the dissolution of less reactive minerals could expose the surfaces of soluble salts present in the agglomerates to dissolution explaining the similar release rates of a number of elements not normally present in silicate minerals (e.g. Cl, SO<sub>4</sub>, and NO<sub>3</sub>).

## 5. Conclusions

A detailed experimental study of the rates of interaction between lake sediments and their coexisting fluids suggest the long-term (hours to months) chemical transfer between sediments and lake waters are dominated by the dissolution of the relatively inert silicate phases like quartz and clay. As a significant percent of sediment grains are agglomerates of both rapidly and slow dissolving minerals, the dissolution of these silicates could expose some more soluble salts, if present in the agglomerates to dissolution. The close correspondence between the dissolution rates of quartz and clay minerals and element release rates measured in this study suggest that laboratory measured silicate dissolution rates can be applied to estimate element fluxes among fluids and sediments in a large number of natural environments.

## Acknowledgments

We would like to thank Jacques Schott, Oleg Pokrovsky, Gleb Pokrovski, Jean-Louis Dandurand, Robert Gout, Stacey Callahan, and Abdelmajid Chouabbi for helpful discussions during the course of this study. Alian Castello, Jean-Claude

Harrichoury, Carole Causserand, Stéphanie Mounic, Carole Boucayrand, Frédéric Candaudap and Thierry Aigouy provided technical assistance. Support from Centre National de la Recherche Scientifique, Ministère de l'Enseignement Supérieur et de la Recherche Scientifique (MESRS-Algeria), Agence Nationale des Barrages (ANB-Algeria) and Agence Nationale des Ressources Hydrauliques (ANRH-Algeria) is gratefully acknowledged.

## References

- Alkattan, M., Oelkers, E.H., Dandurand, J.-L., Schott, J., 1997. Experimental studies of halite dissolution kinetics, 1 the effect of saturation state and the presence of trace metals. *Chem. Geol.* 137, 201–219.
- Brady, P.V., Walther, J.V., 1990. Kinetics of quartz dissolution at low temperatures. *Chem. Geol.* 82, 253–264.
- Brantley, S.L., 2008. Kinetics of mineral dissolution. In: Brantley, S.L., Kubicki, J.D., White, A.F. (Eds.), *Kinetics of water-rock interaction*. Springer, New York, USA, pp. 151–210.
- Brunauer, S., Emmet, P.H., Teller, E., 1938. Adsorption of gases in multi-molecular layers. *J. Am. Chem. Soc.* 60, 309–319.
- Cubillas, P., Köhler, S., Prieto, M., Chaïrat, C., Oelkers, E.H., 2005. Experimental determination of the dissolution rates of calcite, aragonite, and bivalves. *Chem. Geol.* 216, 59–77.
- Dove, P.M., Czank, C.A., 1995. Crystal chemical controls on the dissolution kinetics of the isostructural sulfates: celestite, anglesite, and barite. *Geochim. Cosmochim. Acta* 59, 1907–1915.
- Ganor, J., Lu, P., Zheng, Z., Zhu, C., 2007. Bridging the gap between laboratory experiments and field estimations of weathering using simple equations. *Envir. Geol.* 53, 599–610.
- Gonzalez, A.E., Rodriguez, M.T., Sanchez, J.C., Espinosa, A.J.F., de la Rosa, F.J.B., 2000. Assessment of metals in sediments in a tributary of Guadalquivir River (Spain): Heavy metal partitioning and relation between the water and sediment system. *Water, Air, Soil Pollut.* 121, 11–29.
- Hacini, M., Kherici, N., Oelkers, E.H., 2008. Mineral precipitation rates during the complete evaporation of the Merouane Chott ephemeral lake. *Geochim. Cosmochim. Acta* 72, 1583–1597.
- Harouiya, N., Chaïrat, C., Köhler, S.K., Gout, R., Oelkers, E.H., 2007. The dissolution kinetics and apparent solubility of natural apatite in closed reactors at temperatures from 5 to 50 °C and pH from 1 to 6. *Chem. Geol.* 244, 554–568.
- Hodson, M.E., Langan, S.J., 1999. The influence of soil age on calculated mineral weathering rates. *App. Geochem.* 14, 387–394.
- House, W.A., 2003. Geochemical cycling of phosphorous in rivers. *App. Geochem.* 18, 739–748.
- Huertas, F.J., Chou, L., Wollast, R., 1999. Mechanism of kaolinite dissolution at room temperature and pressure. Part II: Kinetic study. *Geochim. Cosmochim. Acta* 63, 3261–3275.
- Köhler, S.J., Dufaud, F., Oelkers, E.H., 2003. An experimental study of illite dissolution kinetics as a function of pH from 1.4 to 12.4 and temperature from 5 to 50 °C. *Geochim. Cosmochim. Acta* 67, 3583–3594.
- Lijklema, L., 1993. Considerations on modeling the sediment water exchange of phosphorous. *Hydrobiologia* 253, 219–231.
- Maher, K., Steefel, C.I., White, A.F., Stonestrom, D.A., 2009. The role of reaction affinity and secondary minerals in regulating chemical weathering rates at the Santa Cruz Chronosequence, California. *Geochim. Cosmochim. Acta* 73, 2804–2831.
- Oelkers, E.H., 2001. A General kinetic description of multioxide silicate mineral and glass dissolution. *Geochim. Cosmochim. Acta* 65, 3703–3719.
- Oelkers, E.H., Benezeth, P., Pokrovski, G.S., 2009. Thermodynamic databases for water-rock interaction. *Rev. Min. Geochem.* 70, 1–46.
- Owens, P.N., Batallar, J., Collins, A.J., Gomez, B., Hicks, D.M., Horowitz, A.J., et al., 2005. Trustum Fine-grained sediment in river systems: Environmental significance and management. *River. Res. Appl.* 21, 693–717.
- Parkhurst, D.L., Appelo C.A.J., 1999. User's guide to PHREEQC (Version 2) – A computer program for speciation, batch-reaction, one-dimensional transport, and inverse geochemical calculations, U.S. Geol. Surv. Water Res. Inv. (Report 99-4259).
- Plummer, L.N., Wigley, T.M.L., Parkhurst, D.L., 1978. The kinetics of calcite dissolution in CO<sub>2</sub>-water systems at 5 °C and 60 °C and 0.0 to 1.0 atm CO<sub>2</sub>. *Am. J. Sci.* 278, 179–216.
- Rozalen, M.L., Huertas, F.J., Brady, P.V., Cama, J., Garcia, S., Linares, J., 2008. Experimental study of the effect of pH on the kinetics of montmorillonite dissolution at 25 °C. *Geochim. Cosmochim. Acta* 72, 4224–4253.
- Schott, J., Oelkers, E.H., 1995. Dissolution and crystallization rates of silicate minerals as a function of chemical affinity. *Pure Appl. Chem.* 67, 903–910.
- Schott, J., Pokrovsky, O.S., Oelkers, E.H., 2009. The link between mineral dissolution/precipitation kinetics and solution chemistry. *Rev. Min. Geochem.* 70, 207–258.
- Smits, J.G.C., Vandermolen, D.T., 1993. Application of SWITCH, A model for sediment water exchange of nutrients, to Lake Veluwe in the Netherlands. *Hydrobiologia* 253, 281–300.
- Sverdrup, H., 1990. The kinetics of Base Cation Release due to Chemical Weathering. Lund University Press, Lund, Sweden, pp. 226.
- Sverdrup, H., Warfvinge, P., 1993. Calculating field weathering rates using a mechanistic geochemical model-PROFILE. *App. Geochem.* 8, 273–283.
- Vandal, G.M., Fitzerals, W.F., Rolfhus, K.R., Lamborg, C.H., 1995. Modeling the elemental mercury cycle in Palette Lake, Wisconsin, USA. *Water Air Soil Pollut.* 80, 529–538.
- Vila, J.M., 1980. La chaîne alpine d'Algérie orientale et des confins algéro-tunisiens. Thèse d'État, Université Paris-6, pp. 665.
- White, A.F., 1995. Chemical weathering rates of silicate minerals in soils. *Rev. Min.* 31, 407–461.
- White, A.F., Brantley, S.L., 1995. Chemical weathering rates of silicate minerals: An overview. *Rev. Min.* 31, 1–22.
- White, A.F., Brantley, S.L., 2003. The effect of time on the weathering of silicate minerals: Why do weathering rates differ in the laboratory and field? *Chem. Geol.* 202, 497–506.
- Wolfenden, S., Charnock, J.M., Hilton, J., Livens, F.R., Vaughn, D.J., 2005. Sulfide species as a sink for mercury in lake sediments. *Environ. Sci. Tech.* 39, 6644–6648.
- Zhu, C., 2005. In situ feldspar dissolution rates in an aquifer. *Geochim. Cosmochim. Acta* 69, 1435–1453.
- Zhu, C., Lu, P., 2009. Alkali feldspar dissolution and secondary mineral precipitation in batch systems. 3. Saturation states of product minerals and reaction paths. *Geochim. Cosmochim. Acta* 73, 3171–3200.